ACS APPLIED MATERIALS & INTERFACES

Letter

www.acsami.org

# Enhanced Ultraviolet Random Lasing from Au/MgO/ZnO Heterostructure by Introducing p-$Cu_2O$ Hole-Injection Layer

Cen Zhang,[†] Juan Zhang,[†] Weizhen Liu,[*,†,‡] Haiyang Xu,[*,†] Shuai Hou,[†] Chunliang Wang,[†] Liu Yang,[†] Zhongqiang Wang,[†] Xinhua Wang,[‡] and Yichun Liu[†]

[†]Centre for Advanced Optoelectronic Functional Materials Research and Key Laboratory of UV-Emitting Materials and Technology, Ministry of Education, Northeast Normal University, Changchun 130024, China

[‡]State Key Laboratory of Applied Optics, Changchun Institute of Optics, Fine Mechanics and Physics, Chinese Academy of Sciences, Changchun 130033, China

Supporting Information

**ABSTRACT:** Ultraviolet light-emitting devices (LEDs) were fabricated on the basis of Au/MgO/ZnO metal/insulator/semiconductor (MIS) heterostructures. By introducing a thermally oxidized p-type $Cu_2O$ hole-injection layer into this MIS structure, enhanced ultraviolet electroluminescence (EL) and random lasing with reduced threshold injection current are achieved. The enhancement mechanism is attributed to effective hole transfer from p-$Cu_2O$ to i-MgO under forward bias, which increases the initial carrier concentration of MgO dielectric layer and further promotes "impact-ionization" effect induced carrier generation and injection. The current study proposes a new and effective route to improve the EL performance of MIS junction LEDs via introducing extrinsic hole suppliers.

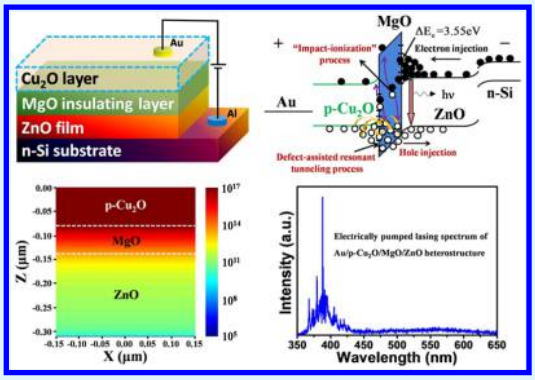


**KEYWORDS:** *Au/MgO/ZnO heterostructure, MIS junction, hole-injection layer, p-type $Cu_2O$, ultraviolet random lasing*

Ultraviolet (UV) light-emitting diodes (LEDs) and lasing diodes (LDs), a very important research topic in modern optoelectronics, have attracted tremendous attentions during the past decades, due to their great application potential in numerous fields such as solid-state lighting, information storage, environment protection and life science.[1−3] ZnO, a typical representative for the third generation semiconductor, is regarded as a promising candidate for low-threshold UV LEDs and LDs because of its wide direct band gap of 3.37 eV and large exciton binding energy of 60 meV.[4−6] However, the lack of high-quality and stable p-type ZnO remains to be the greatest challenge for the development of homojunction devices. Thus, optoelectronic devices comprised of ZnO-based heterostructures arise and exhibit excellent device performance.[7−11] For example, high-brightness blue-light-emitting diode based n-ZnO nanowires/p-GaN film was fabricated and exhibited a high sensitivity in responding to UV irradiation.[12] In addition, one-dimensional ZnO-based heterostructured energy conversion devices are emerging and will be presented for future optoelectronic applications.[13,14] Among them, metal/insulator/semiconductor (MIS) structure is widely adopted to construct LEDs/LDs for wide-band gap semiconductor, because its electroluminescence (EL) mechanism is based on a so-called "impact-ionization" effect, which has no rigid requirements for the p-type counterparts.[11,15−18] In addition, the emission wavelength of this structure will not suffer from a redshift caused by p-type materials.[19] More importantly, electrically pumped lasing action can be more easily achieved with MIS junction structure, because carrier accumulation and population inversion can be facilely fulfilled in the MIS junction, as a result of the blocking effect of dielectric insulating layer. In fact, in the early stage of the development of other wide-band gap semiconductors (e.g., GaN and ZnS), MIS junction diodes were often adopted to achieve the EL (including spontaneous radiation and stimulated emission) from these materials, since their p-type doping was also very difficult at that time.[20,21] Thus, for the research of ZnO-based LEDs and LDs at the present stage, MIS junction structure is still of great importance and practical significance. Figure 1a shows the structural schematic diagram of a typical Au/MgO/ZnO MIS heterostructure and its EL mechanism can be well understood based on the energy band alignment illustrated in Figure 1b. Because of the large conduction band offset (~3.55 eV) between ZnO and MgO, electrons would be blocked and accumulated at the heterostructure interface under forward bias. Most applied voltages would drop on the MgO layer considering its dielectric nature, and the local electric field strength could be as high as $1 \times 10^7$ to $1 \times 10^8$ V/m therein.[11] Thus, electrons and holes can be generated through a so-called "impact-ionization" process in the insulating MgO layer. The

Received: July 20, 2016
Accepted: November 11, 2016
Published: November 11, 2016





DOI: 10.1021/acsami.6b08955
ACS Appl. Mater. Interfaces 2016, 8, 31485−31490

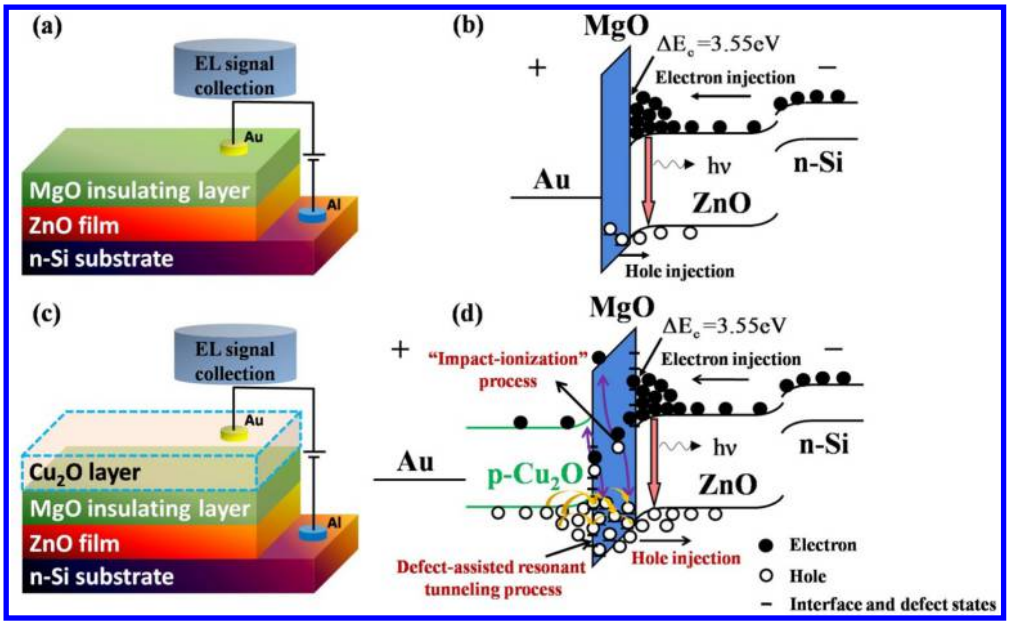


**Figure 1.** (a, b) Structural schematic diagram and corresponding energy-band alignment under forward bias of pristine Au/MgO/ZnO heterostructure, respectively. Herein, the holes are generated through an "impact-ionization" process in the MgO layer and are subsequently driven into the ZnO region under forward bias, where the injected electrons and holes radiatively recombine and UV EL is produced. (c, d) Structural schematic diagram and corresponding energy-band alignment under forward bias of Au/p-$Cu_2O$/MgO/ZnO heterostructure, respectively. The introduction of p-$Cu_2O$ can improve the initial carrier concentration of MgO dielectric layer via effective hole transferring from $Cu_2O$ to MgO, and promote succeeding "impact-ionization" effect induced carrier generation and injection.

generated holes would be driven into ZnO active layer under forward bias and radiatively recombine with the electrons accumulated at ZnO/MgO interface, giving rise to the UV emission of ZnO. Unfortunately, such a kind of "creating something out of nothing" mode seriously limits the EL efficiency of MIS junction LED, because the production of holes via "impact-ionization" effect is not so efficient owing to the extremely low intrinsic carrier concentration ($\sim 1 \times 10^{10}$ $cm^{-3}$ in our case, measured by Hall Effect testing system) in the insulating MgO layer.[22,23] Thus, how to effectively increase the hole generation rate is a key issue for improving the EL performance of ZnO-based MIS heterojunction LEDs. Until now, only a few reports are available on improving the EL performance of ZnO-based MIS junction LEDs,[24−26] especially regarding to LDs. For example, Ma et al. realized the electrically pumped UV random lasing from the Au/$SiO_2$/ZnO MIS heterostructures.[27] Zhu et al. not only achieved electrically pumped random lasers in Au/MgO/ZnO heterostructures, but also effectively reduced the lasing threshold current by inserting a weak p-type (or nearly intrinsic) ZnO film between Au electrode and MgO layer.[11]

In this work, thermally oxidized p-type $Cu_2O$ film, serving as a hole-injection layer, was inserted between metal electrode and dielectric layer to form Au/p-$Cu_2O$/MgO/ZnO heterostructure (see Figure 1c). Under forward bias, the holes from p-type $Cu_2O$ layer can be injected into the MgO deep trap levels via a resonant tunneling process (see Figure 1d). These exotic holes increase the initial carrier concentration of dielectric i-type layer, and favor the "impact-ionization" process under intensive local electric field and make the hole generation and injection into ZnO active region more efficient (see Figure S4 for more detailed discussion). As a consequence, the p-type $Cu_2O$ inserted LED shows improved UV emission and random lasing behavior compared with the pristine Au/MgO/ZnO hetero-structure. Specifically, by introducing p-type $Cu_2O$ hole injection layer, the lasing threshold current was further reduced to nearly half its initial value. To the best of our knowledge, this contribution may be the first time report on improving the electrically pumped random lasing performance of ZnO-based MIS junction diode via introducing p-type $Cu_2O$ film as hole injection layer.

Figure 2a shows the X-ray diffraction (XRD) patterns of these copper-oxide ($Cu_2O$ or CuO) films. Only (111) diffraction peak of $Cu_2O$ was found when the oxidation temperature is 200 °C. As the temperature rises to 275 °C, except for the diffraction signal from the $Cu_2O$ phase, two additional diffraction peaks corresponding to CuO come out. Further increasing oxidation temperature to 400 °C only weakens the $Cu_2O$ signal but enhances the CuO diffraction peaks, indicating a notable phase transition from $Cu_2O$ to CuO at relatively high heating temperature. Thus, to obtain pure-phase $Cu_2O$ film, the optimized oxidation temperature is determined to be 200 °C. Figure 2b exhibits the energy-dispersive X-ray (EDX) spectrum of the $Cu_2O$ film prepared at 200 °C. Only elemental Cu and O signals with an atomic ratio of 1.9:1 were detected, further confirming that the obtained sample is indeed a pure-phase $Cu_2O$ film. The slightly lower Cu content compared to standard stoichiometry is ascribed to the intrinsic copper vacancies existing in $Cu_2O$, which behave as acceptor centers and provide holes for the p-type conductance of $Cu_2O$. Figure 2c summarizes the electrical parameters of the synthesized pure $Cu_2O$ film determined by Hall effect measurement. As can be seen, the $Cu_2O$ film exhibits completely identical p-type conductance at all testing magnetic field intensity. The average hole concentration and Hall mobility are calculated to be $4.5 \times 10^{17}$ $cm^{-3}$ and 0.9 $cm^2/(V\ s)$, respectively. Such good p-type conductivity ensures that the obtained $Cu_2O$ film can play the role of hole-injection layer in the MIS junction LEDs. Figure 2d presents the scanning electron microscopy (SEM) image of the $Cu_2O$ film. It is found


DOI: 10.1021/acsami.6b08955
ACS Appl. Mater. Interfaces 2016, 8, 31485−31490

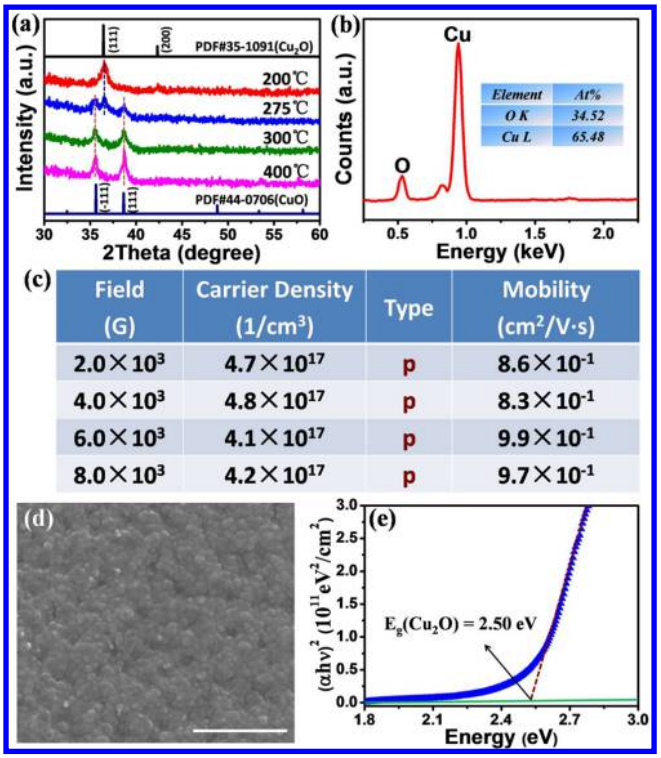


**Figure 2.** (a) XRD patterns of the copper-oxide ($Cu_2O$ or CuO) films obtained at different thermal oxidation temperatures, the curves at the top and bottom are the standard PDF cards for $Cu_2O$ and CuO lattice structures, respectively. (b) EDX spectrum of the pure-phase $Cu_2O$ film prepared at 200 °C, the inset shows the atomic ratio of Cu and O elements. (c) Electrical parameters of the synthesized p-$Cu_2O$ film measured by Hall Effect testing system. (d) Top-view SEM image of the as-prepared $Cu_2O$ granular film; the scale bar is 1 $\mu$m. (e) Optical absorption spectrum of the obtained p-$Cu_2O$ film.

that the prepared sample is a polycrystalline granular film with a mean grain size of ~80 nm. Optical absorption spectrum of the obtained $Cu_2O$ film was measured and plotted in Figure 2e. By extrapolating the linear part of absorption edge, the optical direct band gap of the as-prepared $Cu_2O$ film is estimated to be ~2.50 eV, consistent with the reported values ranging from 2.0 to 2.6 eV by other groups.[28,29]

Figure 3a displays the nearly linear current−voltage ($I$−$V$) relationships between a pair of Al or Au electrodes, which indicates that good ohmic contacts have been formed for Al/n-Si and Au/p-$Cu_2O$. Typical rectifying diode-like behaviors (see Figure 3b) with distinctive turn-on voltages of 5.5 and 2.7 V are observed from both LEDs with and without p-$Cu_2O$ layer, respectively. The larger turn-on bias of p-$Cu_2O$ inserted device is attributed to the increased series resistance from additive $Cu_2O$ film. Besides, compared with the pristine Au/MgO/ZnO heterostructure, p-$Cu_2O$ inserted LED shows a rapider increase of injection current after the device is "turned on". This can be understood in terms of the effective hole transfer from p-$Cu_2O$ to i-MgO (see the next paragraph for detailed discussion), which makes a considerable contribution to the conductive current across the MIS heterojunction.[19]

Figure 4a presents the EL spectra of the MIS junction LED inserted with p-$Cu_2O$ hole-injection layer. As can be seen, an obvious spontaneous emission band centered at 380 nm appears when the injection current is 100 mA. The relatively large injection current may be ascribed to relatively low quality of MgO dielectric layer or the existence of a certain amount of interfacial defects, both of which can lead to a lot of leakage paths in such a MIS heterostructure.[11,17] By comparing with the photoluminescence spectrum of ZnO film (the green dashed line in Figure 4a), the observed UV EL band is attributed to the near-band-edge excitonic recombination in ZnO active layer.[30,31] As the current reaches 200 mA, the entire emission intensity is increased and some sharp peaks arise and superimpose on the spontaneous emission band. With further increase of injection current to 300 and 350 mA, more distinct sharp peaks are observed. The appearance of these sharp peaks demonstrates an electrically pumped lasing action, which is further confirmed by the superlinear dependence of integrated emission intensity on injection current magnitude, as shown in Figure 4b. The lasing threshold current is determined to be ~130 mA. Someone may argue that these emission spikes might be caused by the overheat of metal electrode or probe at high injection currents. However, the heat-induced sharp peaks usually exhibit a broader spectrum coverage range with randomly emerging spikes and irregular variation of emission intensity with injection current (see Figures S1 and S2 for detailed discussion). Obviously, the emission spikes observed in the current experiment do not possess the above-mentioned features of heat-induced sharp peaks. Therefore, the appearance of spikes in the emission spectra is absolutely not induced by the heating effect.

On the contrary, the pristine MIS junction LED without p-$Cu_2O$ layer only exhibits weaker light emission at the same injection currents, and its lasing threshold is estimated to be ~230 mA (see Figure 4c, d). That is, as discussed in the beginning, the p-type $Cu_2O$ inserted device demonstrates the expected better UV emission and electrically pumped lasing

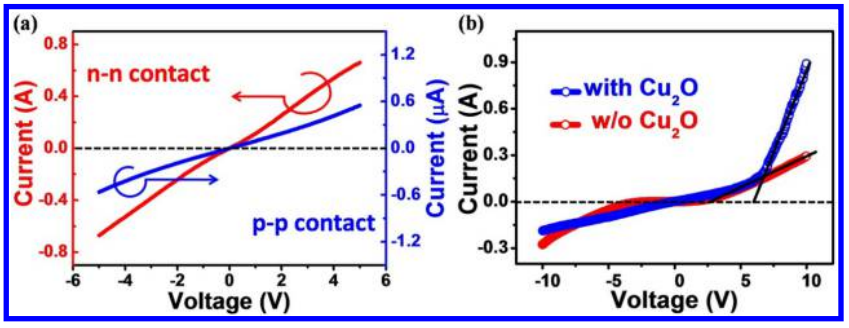


**Figure 3.** (a) Nearly linear $I$−$V$ curves from a pair of Al (red line) or Au (blue line) electrodes, indicating that good ohmic contacts have been formed for Al/n-Si and Au/p-$Cu_2O$. (b) Typical rectifying $I$−$V$ curves from the two LEDs with (blue line) and without (red line) p-$Cu_2O$ layer, respectively.


DOI: 10.1021/acsami.6b08955
ACS Appl. Mater. Interfaces 2016, 8, 31485−31490

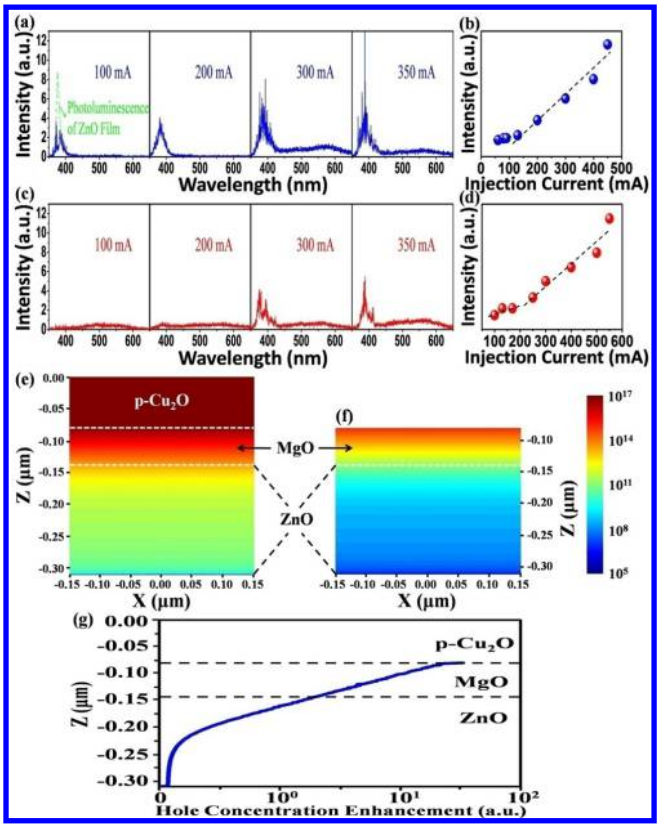


**Figure 4.** (a, c) EL spectra of the Au/MgO/ZnO heterostructures with (blue lines) and without (red lines) p-$Cu_2O$ layer under different injection currents, respectively; the green dashed curve in Figure 4a is the photoluminescence spectrum of ZnO film excited by the 325 nm line of a He−Cd laser. (b, d) Superlinear dependences of integrated emission intensity on the injection current of the two devices with (blue sphere) and without (red sphere) p-$Cu_2O$ layer. (e, f) Simulated distribution profiles of hole concentration in the two LEDs with and without p-$Cu_2O$ layer respectively, which clearly show that the hole concentrations in MgO and ZnO layers are remarkably improved by introducing p-$Cu_2O$ hole injection layer. (g) Hole carrier concentration enhancement after introducing p-$Cu_2O$ hole injection layer.

behavior than the pristine Au/MgO/ZnO heterostructure, thanks to the effective hole transfer from p-$Cu_2O$ to i-MgO under forward bias. Actually, there are some deep-levels at the p-$Cu_2O$/MgO interface, reasonably owing to the lattice mismatch. Therefore, considering the energy band alignment, the holes in p-$Cu_2O$ layer could be injected into MgO by a defect-assisted resonant tunneling process. These exotic holes are accelerated under intensive local electric field and impact the crystal lattice and defect sites in MgO film, that is, facilitate the "impact-ionization" process, generating more excited electrons and holes. Driven by forward bias, these excited holes would tunnel through the junction interface and enter into the ZnO active region, giving out a better UV EL and lasing behavior from the p-type $Cu_2O$ inserted device (as shown in Figure 1d). To support this argument and show the effect of p-$Cu_2O$ layer, analogue simulations of local hole concentration distribution under the same forward applied voltage of 8 V are performed and illustrated in Figures 4e, f. Herein, the simulation software DEVICE 5.0.736 was employed as the calculation tool, and the two simulation architectures were constructed according to the practical device configurations. The insulator (MgO) was assumed to be a p-type semiconductor with very low carrier concentration ($\sim 1 \times 10^{10}$ $cm^{-3}$, similar to the carrier concentration of MgO layer by Hall measurement). The only difference between the two models was the p-$Cu_2O$ layer in one of them. During the simulation, trap-assisted recombination, Auger recombination, and radiative combination of the semiconductors have been taken into account, while the "impact ionization" process was actually not involved because it is a highly nonlinear process, and it is inclusion in the physical model for the semiconductor can easily cause divergences in the simulation. Nonetheless, as can be seen, the overall hole concentration of p-$Cu_2O$ inserted LED is much greater than that of pristine device, indicating the positive role of $Cu_2O$ as an external hole supplier. As shown in Figure 4g, hole concentration enhancement ratio demonstrates that the introduction of p-$Cu_2O$ layer indeed leads to a dramatic increase of hole carrier concentration in MgO insulating layer, MgO/ZnO interface and ZnO active layer, owing to the effective hole transfer and injection from p-$Cu_2O$ to ZnO, which in some extent confirms the EL enhancement mechanism mentioned above. It should be pointed out that this enhancement ratio is not largest at the interface of MgO/ZnO. The reason is that it is regarded as the active region, moreover, the electron concentration is relative higher than the hole concentration at the interface of MgO/ZnO. Reasonably, the hole concentration should reduce gradually during the carrier transport from p-$Cu_2O$ or MgO to the active region owing to the electron−hole recombination processes. By the way, a weak visible emission band peaked at ~560 nm shows up for both LEDs when the electric current is increased. This is because, under high injection level, part of the injected carriers relax to the defect states, giving birth to the observed broadband deep level emission.[32−34]

Finally, let us briefly discuss the mode type and formation mechanism of electrically pumped lasing action. Figure 5a, b show the schematic diagram of angle-dependent EL measurement configuration and the lasing spectra of the p-$Cu_2O$ inserted device recorded from varying detection angles, respectively. Distinct lasing spikes are observed in different directions, which are a strong experimental evidence for random lasing behavior.[11,35] To further prove that the observed phenomenon is electrically pumped random lasing in our experiment, we successively recorded the EL spectra taken from the same device with time interval of 15 s as an alternative. It is found that the lasing spectrum varies with time, as shown in Figure S3. The position and intensity of the observed sharp peaks change randomly, and the mode spacing is not uniform. This is because the feedback path of each closed-loop changes from time to time, which, in turn, results in real-time variations in the collected lasing spectra. This phenomenon reflects the intrinsic properties of random laser oscillation, and can be viewed as another solid evidence for the occurrence of random lasing action in our experiment.[15,18] Figure 5c displays cross-sectional transmission electron microscopy (TEM) image of our ZnO film. As can be seen, the polycrystalline film is composed of many small nanocolumns. Such a kind of relatively disorder system can act as both gain medium and scattering units for random lasing.[15,36] For the device with p-type hole-injection layer, the disordered granular $Cu_2O$ film may even be helpful to the optical confinement of the system by scattering the emitted photons back to the ZnO active layer.[11] When the population inversion condition ($E_{Fn} - E_{Fp} > E_g$) is satisfied (see Figure 5d) and the optical gain is larger than the loss through closed-loop multiscatterings (see Figure 5e), random lasing oscillations occur.


DOI: 10.1021/acsami.6b08955
ACS Appl. Mater. Interfaces 2016, 8, 31485−31490

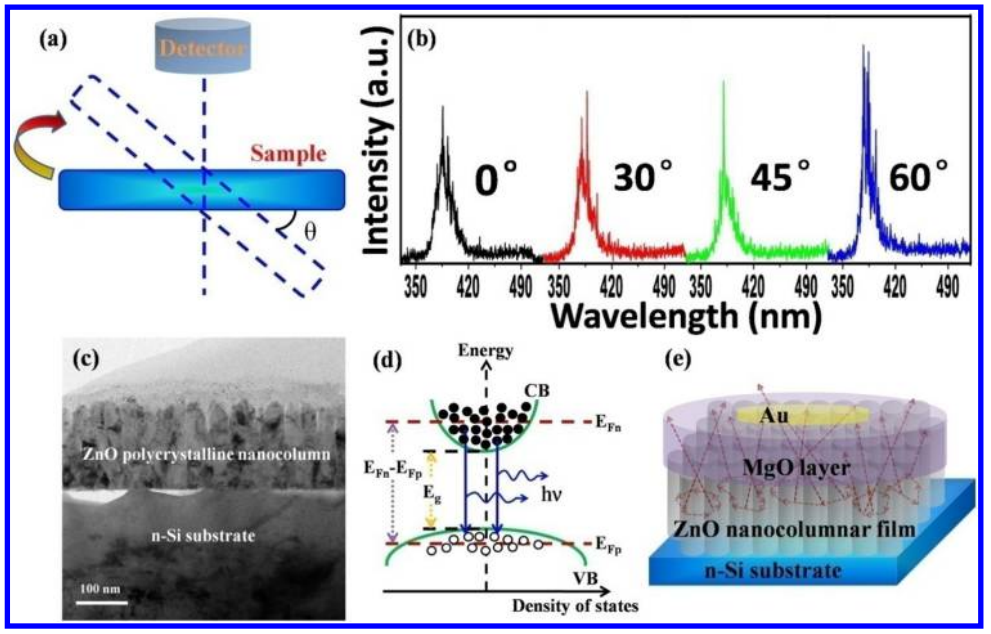


**Figure 5.** (a, b) Schematic diagram of angle-dependent EL measurement configuration and lasing spectra of the p-$Cu_2O$ inserted LD recorded from different detection angles, respectively; herein, the injection current is fixed at 300 mA. (c) Cross-sectional TEM image of the ZnO film prepared by pulsed laser deposition. (d) Schematic process for population inversion and stimulated emission; here, $E_{Fn}$ and $E_{Fp}$ are the quasi-Fermi-levels for electrons in conduction band and holes in valence band, respectively, and $E_g$ is the energy bandgap of ZnO. (e) Schematic illustration of the formation mechanism for random laser via closed-loop multiscatterings process.

In summary, prototype UV LEDs and LDs based on Au/MgO/ZnO heterostructures have been successfully demonstrated. By employing thermally oxidized p-$Cu_2O$ film as hole-injection layer, the UV emission and random lasing performance were dramatically improved. The enhancement mechanism is attributed to the effective hole injection from p-$Cu_2O$ into i-MgO, which increases the initial carrier concentration for "impact-ionization" process and makes the hole generation in i-layer more efficient. Although further optimization of the device efficiency is still needed, the study presented here provides an effective and feasible way to improve the EL performance of MIS junction LEDs/LDs.

## ■ ASSOCIATED CONTENT

### Supporting Information

The Supporting Information is available free of charge on the ACS Publications website at DOI: 10.1021/acsami.6b08955.

Experimental section, discussion on heating effect, successive measurements of lasing spectra, and discussion on energy-band alignment of the Au/p-$Cu_2$/MgO/ZnO heterostructure (PDF)

## ■ AUTHOR INFORMATION

### Corresponding Authors

*E-mail: liuwz455@nenu.edu.cn.

*E-mail: hyxu@nenu.edu.cn.

### Notes

The authors declare no competing financial interest.

## ■ ACKNOWLEDGMENTS

This work is supported by the NSFC for Excellent Young Scholars (51422201), the Program of NSFC (51372035, 51602028, 61505026, and 61604037), "111" Project (No. B13013), Research Fund for the Doctoral Program of Higher Education (20130043110004), the Fund from Jilin Province (No. 20160520009JH, 20160520115JH and 20160520114JH), the 2015 Open Project from State Key Laboratory of Applied Optics (202115002), the China Postdoctoral Science Foundation funded project (2015M580238 and 2016T90237). We thank Dr. Chunyang Liu for his helpful suggestions in revising the manuscript.

## ■ REFERENCES

(1) Yoshida, H.; Yamashita, Y.; Kuwabara, M.; Kan, H. A 342-nm Ultraviolet AlGaN Multiple-Quantum-Well Laser Diode. *Nat. Photonics* **2008**, *2*, 551−554.

(2) Oto, T.; Banal, R. G.; Kataoka, K.; Funato, M.; Kawakami, Y. 100 mW Deep-Ultraviolet Emission from Aluminium-Nitride-Based Quantum Wells Pumped by an Electron Beam. *Nat. Photonics* **2010**, *4*, 767−771.

(3) Li, K. H.; Liu, X.; Wang, Q.; Zhao, S.; Mi, Z. Ultralow-Threshold Electrically Injected AlGaN Nanowire Ultraviolet Lasers on Si Operating at Low Temperature. *Nat. Nanotechnol.* **2015**, *10*, 140−144.

(4) Ni, P.-N.; Shan, C.-X.; Li, B.-H.; Wang, S.-P.; Shen, D.-Z. Bias-Polarity Dependent Ultraviolet/Visible Switchable Light-Emitting Devices. *ACS Appl. Mater. Interfaces* **2014**, *6*, 8257−8262.

(5) Fang, X.; Wei, Z.; Yang, Y.; Chen, R.; Li, Y.; Tang, J.; Fang, D.; Jia, H.; Wang, D.; Fan, J.; Ma, X.; Yao, B.; Wang, X. Ultraviolet Electroluminescence from ZnS@ZnO Core-Shell Nanowires/p-GaN Introduced by Exciton Localization. *ACS Appl. Mater. Interfaces* **2016**, *8*, 1661−1666.

(6) Chu, S.; Wang, G.; Zhou, W.; Lin, Y.; Chernyak, L.; Zhao, J.; Kong, J.; Li, L.; Ren, J.; Liu, J. Electrically Pumped Waveguide Lasing from ZnO Nanowires. *Nat. Nanotechnol.* **2011**, *6*, 506−510.

(7) Huang, J.; Chu, S.; Kong, J.; Zhang, L.; Schwarz, C. M.; Wang, G.; Chernyak, L.; Chen, Z.; Liu, J. ZnO p-n Homojunction Random Laser Diode Based on Nitrogen-Doped p-type Nanowires. *Adv. Opt. Mater.* **2013**, *1*, 179−185.

(8) Liu, W.; Wang, W.; Xu, H.; Li, X.; Yang, L.; Ma, J.; Liu, Y. Bias-Bolarity-Dependent UV/Visible Transferable Electroluminescence from ZnO Nanorod Array LED with Graphene Oxide Electrode Supporting Layer. *Appl. Phys. Express* **2015**, *8*, 095202.

(9) Liu, W.; Xu, H.; Yan, S.; Zhang, C.; Wang, L.; Wang, C.; Yang, L.; Wang, X.; Zhang, L.; Wang, J.; Liu, Y. Effect of $SiO_2$ Spacer-Layer Thickness on Localized Surface Plasmon-Enhanced ZnO Nanorod Array LEDs. *ACS Appl. Mater. Interfaces* **2016**, *8*, 1653−1660.
(10) Zhu, H.; Shan, C.-X.; Yao, B.; Li, B.-H.; Zhang, J.-Y.; Zhang, Z.-Z.; Zhao, D.-X.; Shen, D.-Z.; Fan, X.-W.; Lu, Y.-M.; Tang, Z.-K. Ultralow-Threshold Laser Realized in Zinc Oxide. *Adv. Mater.* **2009**, *21*, 1613−1617.
(11) Zhu, H.; Shan, C.-X.; Zhang, J.-Y.; Zhang, Z.-Z.; Li, B.-H.; Zhao, D.-X.; Yao, B.; Shen, D.-Z.; Fan, X.-W.; Tang, Z.-K.; Hou, X.; Choy, K.-L. Low-Threshold Electrically Pumped Random Lasers. *Adv. Mater.* **2010**, *22*, 1877−1881.
(12) Zhang, X.-M.; Lu, M.-Y.; Zhang, Y.; Chen, L.-J.; Wang, Z. L. Fabrication of a High-Brightness Blue-Light-Emitting Diode Using a ZnO-Nanowire Array Grown on p-GaN Thin Film. *Adv. Mater.* **2009**, *21*, 2767−2770.
(13) Zhang, Y.; Yang, Y.; Gu, Y.; Yan, X.; Liao, Q.; Li, P.; Zhang, Z.; Wang, Z. Performance and Service Behavior in 1-D Nanostructured Energy Conversion Devices. *Nano Energy* **2015**, *14*, 30−48.
(14) Zhang, Z.; Liao, Q.; Yu, Y.; Wang, X.; Zhang, Y. Enhanced Photoresponse of ZnO Nanorods-Based Self-Powered Photodetector by Piezotronic Interface Engineering. *Nano Energy* **2014**, *9*, 237−244.
(15) Liu, C. Y.; Xu, H. Y.; Ma, J. G.; Li, X. H.; Zhang, X. T.; Liu, Y. C.; Mu, R. Electrically Pumped Near-Ultraviolet Lasing from ZnO/MgO Core/Shell Nanowires. *Appl. Phys. Lett.* **2011**, *99*, 063115.
(16) Li, Y.; Ma, X.; Jin, L.; Yang, D. A Chemical Strategy to Reinforce Electrically Pumped Ultraviolet Random Lasing from ZnO Films. *J. Mater. Chem.* **2012**, *22*, 16738−16741.
(17) Ni, P. N.; Shan, C. X.; Wang, S. P.; Lu, Y. J.; Li, B. H.; Shen, D. Z. Fabry-Perot Resonance Enhanced Electrically Pumped Random Lasing from ZnO Films. *Appl. Phys. Lett.* **2015**, *107*, 231108.
(18) Liu, C. Y.; Xu, H. Y.; Sun, Y.; Ma, J. G.; Liu, Y. C. ZnO Ultraviolet Random Laser Diode on Metal Copper Substrate. *Opt. Express* **2014**, *22*, 16731−16737.
(19) Lu, Y.-J.; Shan, C.-X.; Zhou, Z.-X.; Wang, Y.-L.; Li, B.-H.; Qin, J.-M.; Ma, H.-A.; Jia, X.-P.; Chen, Z.-H.; Shen, D.-Z. Electrically Pumped Random Lasers with p-diamond as a Hole Source. *Optica* **2015**, *2*, 558−562.
(20) Lagerstedt, O.; Monemar, B.; Gislason, H. Properties of GaN Tunneling MIS Light-Emitting Diodes. *J. Appl. Phys.* **1978**, *49*, 2953−2957.
(21) Walker, L. G.; Pratt, G. W. Low-Voltage Tunnel-Injection Blue Electroluminescence in ZnS MIS Diodes. *J. Appl. Phys.* **1976**, *47*, 2129−2133.
(22) Mitoff, S. P. Electrical Conductivity of Single Crystals of MgO. *J. Chem. Phys.* **1959**, *31*, 1261−1269.
(23) Wu, R. Q.; Shen, L.; Yang, M.; Sha, Z. D.; Cai, Y. Q.; Feng, Y. P.; Huang, Z. G.; Wu, Q. Y. Enhancing Hole Concentration in AlN by Mg:O Codoping: Ab Initio Study. *Phys. Rev. B: Condens. Matter Mater. Phys.* **2008**, *77*, 073203.
(24) Jung, B. O.; Lee, J. H.; Lee, J. Y.; Kim, J. H.; Cho, H. K. High-Purity Ultraviolet Electroluminescence from n-ZnO Nanowires/$p^+$-Si Heterostructure LEDs with i-MgO Film as Carrier Control Layer. *J. Electrochem. Soc.* **2012**, *159*, H102−H106.
(25) Mo, X.; Fang, G.; Long, H.; Li, S.; Wang, H.; Chen, Z.; Huang, H.; Zeng, W.; Zhang, Y.; Pan, C. Unusual Electroluminescence from n-ZnO@i-MgO Core-Shell Nanowire Color-Tunable Light-Emitting Diode at Reverse Bias. *Phys. Chem. Chem. Phys.* **2014**, *16*, 9302−9308.
(26) Shi, Z.-F.; Zhang, Y.-T.; Cui, X.-J.; Zhuang, S.-W.; Wu, B.; Jiang, J.-Y.; Chu, X.-W.; Dong, X.; Zhang, B.-L.; Du, G.-T. Epitaxial Growth of Vertically Aligned ZnO Nanowires for Bidirectional Direct-Current Driven Light-Emitting Diodes Applications. *CrystEngComm* **2015**, *17*, 40−49.
(27) Ma, X.; Pan, J.; Chen, P.; Li, D.; Zhang, H.; Yang, Y.; Yang, D. Room Temperature Electrically Pumped Ultraviolet Random Lasing from ZnO Nanorod Arrays on Si. *Opt. Express* **2009**, *17*, 14426−14433.
(28) Pearton, S. J.; Abernathy, C. R.; Overberg, M. E.; Thaler, G. T.; Norton, D. P.; Theodoropoulou, N.; Hebard, A. F.; Park, Y. D.; Ren, F.; Kim, J.; Boatner, L. A. Wide Band Gap Ferromagnetic Semiconductors and Oxides. *J. Appl. Phys.* **2003**, *93*, 1−13.
(29) Nakano, Y.; Saeki, S.; Morikawa, T. Optical Bandgap Widening of p-type $Cu_2O$ Films by Nitrogen Doping. *Appl. Phys. Lett.* **2009**, *94*, 022111.
(30) Wei, Z. P.; Lu, Y. M.; Shen, D. Z.; Wu, C. X.; Zhang, Z. Z.; Zhao, D. X.; Zhang, J. Y.; Fan, X. W. Effect of Interface on Luminescence Properties in ZnO/MgZnO Heterostructures. *J. Lumin.* **2006**, *119*−*120*, 551−555.
(31) Wang, X.; Lu, Y. M.; Shen, D. Z.; Zhang, Z. Z.; Li, B. H.; Yao, B.; Zhang, J. Y.; Zhao, D. X.; Fan, X. W. Growth and Photoluminescence for Undoped and N-doped ZnO Grown on 6H-SiC Substrate. *J. Lumin.* **2007**, *122*−*123*, 165−167.
(32) Dai, J.; Xu, C. X.; Sun, X. W. ZnO-Microrod/p-GaN Heterostructured Whispering-Gallery-Mode Microlaser Diodes. *Adv. Mater.* **2011**, *23*, 4115−4119.
(33) Yang, Q.; Wang, W.; Xu, S.; Wang, Z. L. Enhancing Light Emission of ZnO Microwire-Based Diodes by Piezo-Phototronic Effect. *Nano Lett.* **2011**, *11*, 4012−4017.
(34) Choi, S.; Berhane, A. M.; Gentle, A.; Ton-That, C.; Phillips, M. R.; Aharonovich, I. Electroluminescence from Localized Defects in Zinc Oxide: Toward Electrically Driven Single Photon Sources at Room Temperature. *ACS Appl. Mater. Interfaces* **2015**, *7*, 5619−5623.
(35) Long, H.; Fang, G.; Li, S.; Mo, X.; Wang, H.; Huang, H.; Jiang, Q.; Wang, J.; Zhao, X. A ZnO/ZnMgO Multiple-Quantum-Well Ultraviolet Random Laser Diode. *IEEE Electron Device Lett.* **2011**, *32*, 54−56.
(36) Gottardo, S.; Cavalieri, S.; Yaroshchuk, O.; Wiersma, D. S. Quasi-Two-Dimensional Diffusive Random Laser Action. *Phys. Rev. Lett.* **2004**, *93*, 263901.


DOI: 10.1021/acsami.6b08955
*ACS Appl. Mater. Interfaces* 2016, 8, 31485−31490